Journal of Colloid and Interface Science 475 (2016) 26–35

Contents lists available at ScienceDirect

Journal of Colloid and Interface Science

journal homepage: www.elsevier.com/locate/jcis

# Influence of metal oxides on the adsorption characteristics of PPy/metal oxides for Methylene Blue

Jie Chen, Jiangtao Feng *, Wei Yan *

*Department of Environmental Science and Engineering, State Key Laboratory of Multiphase Flow in Power Engineering, Xi'an Jiaotong University, Xi'an 710049, PR China*

## GRAPHICAL ABSTRACT

The metal oxides influenced the PPy adsorption characteristics in following factors: (1) Zeta potential, the PPy content, textural properties, and morphology of composite. (2) The affinity of their composites with MB.

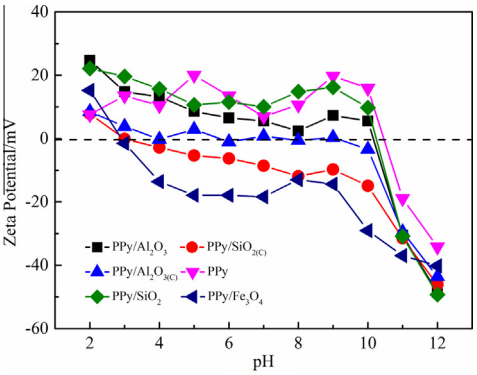


## ARTICLE INFO

*Article history:*
Received 23 February 2016
Revised 9 April 2016
Accepted 12 April 2016
Available online 22 April 2016

*Keywords:*
Polypyrrole/metal oxide composites
$SiO_2$
$Al_2O_3$
$Fe_3O_4$
Influence investigation
Methylene blue adsorption

## ABSTRACT

In this paper, the pure PPy and PPy/metal oxide composites including PPy/$SiO_2$, PPy/$Al_2O_3$, and PPy/$Fe_3O_4$ as well as PPy coated commercial $SiO_2$ and $Al_2O_3$ (PPy/$SiO_{2(C)}$ and PPy/$Al_2O_{3(C)}$) were successfully synthetized via chemical oxidative polymerization in acid aqueous medium to investigate the influence of metal oxides on adsorption capacity and their adsorption characteristics for Methylene Blue (MB). The composites were characterized by Zeta potential analysis, BET analysis, X-ray diffraction (XRD), Fourier transform infrared spectroscopy (FT-IR), thermogravimetric analysis (TGA) and scanning electron microscope (SEM). The results indicate that the metal oxides have great impact on textural properties, morphology, Zeta potential and PPy polymerization on their surface, further influence the adsorption capacity of their composites. The PPy/$Al_2O_{3(C)}$ composite owns the highest specific surface area, rougher surface and most PPy content, and show the highest monolayer adsorption capacity reaching 134.77 mg/g. In the adsorption characteristic studies, isotherm investigation shows an affinity order of PPy/metal oxides of PPy/$Al_2O_{3(C)}$ > PPy/$Al_2O_3$ > PPy/$SiO_{2(C)}$ > PPy/$SiO_2$ > PPy/$Fe_3O_4$ > PPy, stating the affinity between PPy and MB was greatly improved by metal oxide, and $Al_2O_3$ owns high affinity for MB, followed by $SiO_2$ and $Fe_3O_4$. Kinetic data of the composites selected (PPy/$SiO_{2(C)}$, PPy/$Al_2O_{3(C)}$ and PPy/$Fe_3O_4$) were described more appropriately by the pseudo-second-order model, and the order of $K_2$ is PPy/

* Corresponding authors.
*E-mail addresses:* fjtes@mail.xjtu.edu.cn (J. Feng), yanwei@mail.xjtu.edu.cn (W. Yan).

http://dx.doi.org/10.1016/j.jcis.2016.04.017
0021-9797/

$Al_2O_3$ > PPy/$SiO_2$ > PPy/$Fe_3O_4$, further showing a fast adsorption and good affinity of PPy/$Al_2O_{3(C)}$ for MB. The regeneration method by HCl-elution and NaOH-activation was available, and the composites selected still owned good adsorption and desorption efficiency after six adsorption-desorption cycles.


## 1. Introduction

The environmental pollutions caused by MB, which is widely used in pesticides, rubbers, varnishes, pharmaceuticals and dyestuffs, have drawn much attention in recent years [1]. MB have resistance to degrade by bio-method, chemical oxidation and photocatalytic degradation because of their complex aromatic molecular properties, thus influencing photosynthetic processes of aquatic plants and the oxygen levels in water [2–4]. Meanwhile, MB is toxic and carcinogenic that can cause irritation, allergy and cancer in humans [5]. As a result, proper treatment methods for MB such as adsorption [6], membrane filtration [7], flocculation [8], chemical oxidation [9] and electrolysis [10] have been proposed in recent years. Adsorption, which is regarded as an excellent treatment method with many advantages such as low capital investment, abundant raw material source, simple in design and operation, and non-toxic, is favored by many investigators [11]. Several groups have reported some adsorbents of dye including activated carbon, fly ash, zeolite, metal oxides, peats, red mud and polymers [12]. However, the adsorbents reported receive many drawbacks such as high cost of investment and operating, regeneration difficulty, and long time to achieve adsorption equilibrium, thus restricting the application employing adsorption method in dye removing in large scale. Therefore, investigations of new recyclable adsorbents are emergent to be conducted [13,14].

Recently, many investigators focus on the conducting polymer polypyrrole (PPy) in various research fields due to its good electrical conductivity, relatively high air stability, low cost, and useful properties for fabricating nano-structured material. PPy may own the adsorption ability through ion exchange or electrostatic interaction though the nitrogen atom which is positively charged in PPy matrix [15–17]. When it is treated with acid or alkali solution, PPy can proceed protonation or deprotonation processes, resulting in doping or dedoping of counter ions [18]. Thanks to the reversible transformation capability, adsorbents based on PPy can be regenerated in the adsorption. However, many adsorbents reported have poor regeneration ability, resulting in high treatment cost. Thus, PPy may have good application prospects as a recyclable adsorbent. The combination of polymers and metal oxides used as adsorbents have received their extensive attention over the past decade [19]. Many low cost metal oxides such as $SiO_2$, $Al_2O_3$ and $Fe_3O_4$, which owns abundant of function groups on the surface, have been used specifically for synthesis of many polymer composite, and the specific surface area and adsorption capacity of polymers were improved intensively. In addition, the particle size and weight of the combined composites are more suitable for collection, thus creating a good condition for engineering application without the size limitation [20]. For these reasons, the composites combined polymers with these metal oxides may receive wide attentions in many fields. Li et al. [20,21] synthetized the polypyrrole-modified $TiO_2$ composite adsorbent, and applied it to adsorb acid red G and MB. The results show the composite had stable performance for dyes adsorption. As is known to all, the separation of adsorbents from the solution is difficult in the application. However, $Fe_3O_4$, which is super paramagnetic and shows high recovery ability than $TiO_2$, have not been applied in PPy/$Fe_3O_4$ for MB adsorption. Moreover, it's important that the properties of metal oxide carriers may have great impact on the adsorption characteristics of PPy for MB. Even though there were various literatures concerning PPy/metal oxides for MB removal, few efforts had been paid on the intensive study about how metal oxides influence the adsorption characteristics of PPy for MB. Furthermore, few literatures were conducted to investigate the adsorption characteristics for MB of PPy/$SiO_2$, PPy/$Al_2O_3$ and PPy/$Fe_3O_4$. Thus, the aim of this work is to intensively study the influence of metal oxides including $SiO_2$, $Al_2O_3$, and $Fe_3O_4$ on adsorption capacity and their adsorption characteristics for MB.

In this paper, different metal oxides with different textural properties and morphology ($SiO_2$, $Al_2O_3$ and $Fe_3O_4$) coated with polypyrrole were synthesized. The composites were characterized by Zeta potential analysis, BET analysis, X-ray diffraction (XRD), Fourier transform infrared spectroscopy (FT-IR), thermogravimetric analysis (TGA) and scanning electron microscope (SEM). Batch adsorption experiments were conducted to investigate the effect of surface potential and ionic strength on the MB removal efficiency. Their adsorption characteristics such as adsorption capacity, adsorption isotherm and kinetic to MB were also studied, and the influence mechanisms of metal oxides on the adsorption capacity for MB of composite were summarized. Moreover, we evaluated the regenerate capacity and adsorption mechanism to provide a confidence that the composites have bright prospects in dye wastewater treatment.

## 2. Experimental

### 2.1. Materials

Pyrrole (98%) acquired from Zhejiang Qingquan Pharmaceutical & Chemical Ltd. was distilled twice, and then stored in the dark under nitrogen. $SiO_2$ and $Al_2O_3$ powder were obtained from Guangzhou HuaLiSen Trade Co., China. Methylene Blue (MB) was purchased from Beijing Chemical Reagent Co., China. Other chemicals, including $NH_3{\cdot}H_2O$ (25%), $FeCl_3$, NaOH, HCl, citric acid, $Na_2SO_4$, $Al_2SO_4$, $AlCl_3$, $FeCl_2$, $FeCl_3$, anhydrous ethanol, tetraethyl orthosilicate and carbamide were of analytical reagent grades and used without further purification. The deionized water was gained by EPED-40TF Superpure Water System (EPED, China).

### 2.2. Synthesis of metal oxides ($SiO_2$, $Al_2O_3$ and $Fe_3O_4$)

The $SiO_2$ powder was synthesized by the sol-gel method. 146 mL $C_2H_5OH$ and 3 mL deionized water were dispersed in 10 mL $NH_3{\cdot}H_2O$, and then 7 mL tetraethyl orthosilicate was added before being stirred for 6 h. The $SiO_2$ powder was filtrated and washed with deionized water, and dried completely in the electric thermostatic drying oven at a constant temperature of 50 °C.

The $Al_2O_3$ powder was gained by mixing 2.67 g $Al_2SO_4$ and 0.267 g $AlCl_3$ with 200 mL deionized water. Then 7.2 g carbamide was added into the mixture after being mixed uniformly. The mixture was stirred at a constant temperature of 90 °C until white deposits produced, and then the sample was matured at room temperature for 24 h. After that, the sample was filtrated and washed with deionized water and dried completely at a constant temperature of 50 °C.

The $Fe_3O_4$ powder was obtained by adding 1.72 g $FeCl_2$ and 5.06 g $FeCl_3$ in 200 mL deionized water. The mixture was stirred

at a constant temperature of 90 °C before 10 mL $NH_3{\cdot}H_2O$ was added. And the solid was filtrated and washed with deionized water and dried completely at a constant temperature of 50 °C.

### 2.3. Synthesis of adsorbents

The commercial $SiO_2$ and $Al_2O_3$ which own different textural and surface properties with that of pre-prepared $SiO_2$ and $Al_2O_3$ were also used. The composites were synthesized by the chemical oxidative polymerization of pyrrole monomer with the pre-prepared ($SiO_2$, $Al_2O_3$ and $Fe_3O_4$) or commercial ($SiO_2$ and $Al_2O_3$) powdered metal oxide. The process was described as follows. First, a certain amount of five different metal oxides were dispersed in 200 mL deionized water, respectively, and the formed suspension solution was cooled to 5 °C, followed by adding 0.675 mL of pyrrole monomer with stirring for 30 min. After that, 25 mL $FeCl_3$ (3.0 mol/L) solution was added dropwise to the mixed solution of metal oxides, pyrrole monomer and deionized water, and then the solution was stirred for another 24 h. Finally, the composites were filtrated and washed with deionized water. The composites based on prepared $Fe_3O_4$, $SiO_2$, $Al_2O_3$ and commercial $SiO_2$, $Al_2O_3$, named as PPy/$Fe_3O_4$, PPy/$SiO_2$, PPy/$Al_2O_3$, PPy/$SiO_{2(C)}$ and PPy/$Al_2O_{3(C)}$ according to the type of metal oxides, were dried at 50 °C for 24 h. For comparison, the PPy was also synthesized with the same procedure.

### 2.4. Characterization

The Zeta potentials of samples were acquired on a Malvern Zetasizer Nano ZS90. The composites were pre-prepared by adding 5 mg of sample in a 10 mL $10^{-3}$ mol/L NaCl solution at different pH values with $HNO_3$ or NaOH. The BET surface areas ($S_{BET}$) were measured at 77 K using Builder SSA-4200 (Beijing, China). The X-ray diffraction pattern of composites was acquired by Cu Kα radiation on an X'Pert PRO MRD Diffractometer. The Fourier transform infrared spectra (FT-IR) of samples were obtained on a BRUKER TENSOR 37 FT-IR spectrophotometer by the KBr pellet method in the range of 4000–400 $cm^{-1}$. The thermogravimetric (TG) analyses were kept at a heating rate of 10 °C/min in $N_2$ flow, and performed on Setaram Labsys Evo. The sample morphology was characterized by scanning electron microscopy (SEM, JSM-6700F, Japan). The concentration of MB solutions in this study was analyzed by an Agilent 8453 UV–vis spectrophotometer (665 nm).

### 2.5. Batch adsorption experiments

In order to improve the adsorption capacity of adsorbents, the adsorbents were pretreated by 5 mL HCl or NaOH solutions (pH = 1.0–13.0) for 20 min [20]. The batch adsorption experiments were all performed under this optimized condition. The adsorption capacity was calculated according to the equation as follows:

$$q_e = \frac{(C_0 - C_e)V}{m}, \tag{1}$$

where $m$ (g) is the weight of adsorbent applied, and $V$ (L) is the solution volume. $q_e$ (mg/g) is the adsorption amount at equilibrium state. $C_0$ and $C_e$ (mg/L) are the concentrations of MB at initial and equilibrium state.

In the experiments of effect of surface potential and ionic strength, 0.04 g composites were pretreated and added into 20 mL 300 mg/L MB solution before being stirred for 120 min at a constant temperature of 25 °C in dark. Then the suspension was centrifuged or using a hand held magnet at 4000 rpm for 5 min to separate the adsorbent with solution. Meanwhile, in order to study the influence of the adsorbent surface potential on the adsorption capacities, the adsorbents were pretreated by HCl or NaOH solutions (pH = 1.0–13.0) for 20 min before adsorption. The influence of ionic concentration (0–0.3 mol/L) on the adsorption was carried out by adding $Na_2SO_4$ into 300 mg/L MB solution.

The adsorption isotherm is an important basis for the study of adsorption process. In the isotherm experiments, 0.04 g composites were pretreated and added into 20 mL different concentrations (50–400 mg/L) of MB solutions before being stirred for 120 min at a constant temperature of 25 °C in dark. Then the suspension was centrifuged or using a hand held magnet at 4000 rpm for 5 min to separate the adsorbent with solution. Two conventional adsorption isotherm models are the Langmuir and Freundlich isotherm models. The Langmuir model was mainly based on the assumption as follows: (1) it's a monomolecular layer adsorption process; (2) all the adsorption sites are totally equivalent, and only one molecule can be fixed on an adsorption site; (3) the adsorbed molecules were independent [22–24]. On the contrary, the Freundlich model is an empirical equation based on the assumption that the surfaces of the adsorbents were heterogeneous, and various kinds of adsorption sites existed, making it to be more appropriate to describe practical adsorption process [25]. They can be described as follows:

(Langmuir isotherm)

$$\frac{C_e}{q_e} = \frac{1}{q_m K_L} + \frac{1}{q_m} C_e, \tag{2}$$

(Freundlich isotherm)

$$\lg q_e = \lg K_F + \frac{1}{n} \lg C_e, \tag{3}$$

where $q_e$ (mg/g) is the adsorption capacity, which usually refers to the quality of the solvent adsorbed per unit mass of adsorbent; $q_m$ (mg/g) is the maximum adsorption capacity; $C_e$ (mg/L) is the concentration of MB when the adsorption process equilibrium is achieved; $K_L$ ($mg^{1-n}{\cdot}L^n/L$) and $K_F$ (L/mg) are constants of Langmuir and Freundlich, respectively.

Kinetic studies were carried out at 25 °C with three initial concentrations of MB solutions (100, 300, 400 mg/L) in various contact time (0–180 min). The pseudo-first-order model relating to the physical diffusion, and pseudo-second-order model used to determine whether the adsorption rate is controlled by chemisorption mechanism, are applied extensively to analyze the kinetic data [26]. The pseudo-first-order model is arranged and described as follows:

$$\lg(q_e - q_t) = \lg q_e - K_1 t, \tag{4}$$

where $t$ (min) is the adsorption time; $q_t$ (mg/g) is the adsorption amount at some time t; $K_1$ ($min^{-1}$) is a constant of the diffusion rate, and $q_e$ and $K_1$ can be obtained from the fitting equation by analyzing the plot of $\lg(q_e\text{-}q_t)$ versus $t$. The pseudo-second-order model can be arranged and described as follows:

$$\frac{t}{q_t} = \frac{1}{K_2 q_e^2} + \frac{1}{q_e} t, \tag{5}$$

where $K_2$ (g/(mg min)) is the rate constant of the pseudo-second-order model. $q_e$ and $K_2$ can be obtained from the fitting equation by analyzing the plot of $t/q_t$ versus $t$.

In the regeneration study, 300 mg/L MB solutions were used in the regeneration investigations in dark, and the contact time was 3 h. Then 20 mL, 1 mol/L HCl was applied separately as regeneration agents to release MB for 60 min. Then the concentrations of MB after adsorption were measured and calculated after 5 min centrifugation. The adsorption and desorption efficiency (%) were obtained according to the following equations:

$$\text{Removal efficiency} = \frac{C_0 - C_e}{C_0} \times 100\% \tag{6}$$

$$\text{Regeneration efficiency} = \frac{q_d}{q_a} \times 100\% \quad (7)$$

where $q_d$ (mg/g) is the desorbed amount of MB released in the elution agents, $q_a$ (mg/g) is the adsorbed amount of MB on the composites.

## 3. Result and discussion

### 3.1. Characterization of the samples

The FT-IR spectra and their assignments are shown in Fig. S1. The 1560 and 1460 $cm^{-1}$ bands are ascribed to C—C and C—N stretching vibration of the pyrrole ring, respectively. The bands at 1180 $cm^{-1}$ belonging to C—H or C—N in-plane deformation vibration, while the peak situated around in 1080 and 1049 $cm^{-1}$ attributing to C—H or N—H in-plane deformation vibration of the polypyrrole are detected in the spectra, conforming that existence of polypyrrole [27–29]. All metal oxides typical bands in the composites at 470, 1098 $cm^{-1}$ ($SiO_2$) [30], 532 $cm^{-1}$ ($Al_2O_3$) [31] and 500–600 $cm^{-1}$ ($Fe_3O_4$) [23] were also found, demonstrating that the composites were synthetized successfully.

Fig. 1 denotes X-ray diffraction patterns of the six studied composites. The XRD patterns of the composites, except PPy/$Fe_3O_4$, are dominant amorphous structures, which are the same with that of the pure PPy, showing that the metal oxide particles are coated by the amorphous PPy matrix. Diffraction peak at about 25°, which is attributed to the characteristic diffraction peak of PPy, slightly shifts in the XRD pattern of the PPy/metal oxide composites, suggesting that PPy coated on the metal oxides chemically [32]. The diffraction peaks at 30.28° (2 2 0), 35.46° (3 1 1), 43.40° (4 0 0), 53.28° (4 2 2), 57.14° (5 1 1) and 62.76° (4 4 0) which are consistent with the database of $Fe_3O_4$ in JCPDS file (PCPDFWIN v.2.02, PDF NO. 85-1436) are detected in the pattern of PPy/$Fe_3O_4$, showing that the core of composite is pure $Fe_3O_4$ phase with a spinal structure [29].

The textural properties of PPy, $Fe_3O_4$, $Al_2O_3$, $Al_2O_{3(C)}$, $SiO_2$, $SiO_{2(C)}$, PPy/$Fe_3O_4$, PPy/$Al_2O_3$, PPy/$Al_2O_{3(C)}$, PPy/$SiO_2$ and PPy/$SiO_{2(C)}$ are listed in Table 1. It shows that the composites have much larger total pore volume ($V$), average pore radius ($R$) and specific surface area ($S_{BET}$) than that of pure PPy, revealing the great benefit of metal oxides. The results also show that different PPy/metal oxides have different textural properties, indicating that the textural of PPy/metal oxides have great relationship with that of metal oxides. Compared with that of their corresponding metal oxides, the total pore volume, average pore radius and specific surface area decreased after modification, which owning to the block of PPy on the pores.

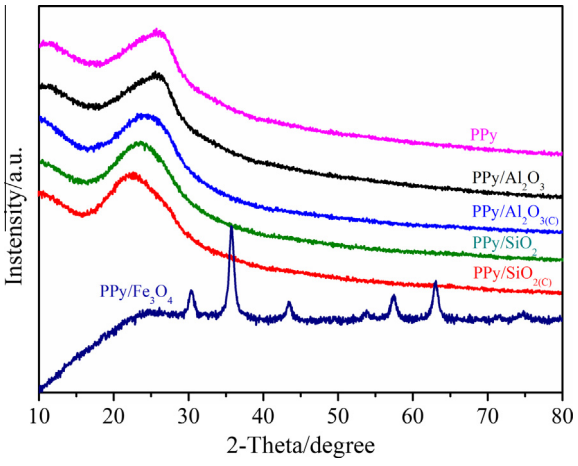


**Fig. 1.** XRD patterns of the PPy/metal oxide composites.

**Table 1**
The textural parameters of the PPy/metal oxide composites.

| Composites | $S_{BET}$ ($m^2$/g) | $V$ ($cm^3$/g) | $R$ (Å) |
|---|---|---|---|
| PPy | 6.35 | 0.04 | 148.8 |
| $Fe_3O_4$ | 75.63 | 0.36 | 81.2 |
| PPy/$Fe_3O_4$ | 65.57 | 0.26 | 79.9 |
| $Al_2O_3$ | 60.24 | 0.23 | 125.3 |
| PPy/$Al_2O_3$ | 41.71 | 0.18 | 124.6 |
| $Al_2O_{3(C)}$ | 350.15 | 0.42 | 26.6 |
| PPy/$Al_2O_{3(C)}$ | 328.67 | 0.39 | 23.9 |
| $SiO_2$ | 60.58 | 0.35 | 113.3 |
| PPy/$SiO_2$ | 46.77 | 0.24 | 112.6 |
| $SiO_{2(C)}$ | 69.87 | 0.29 | 119.3 |
| PPy/$SiO_{2(C)}$ | 56.61 | 0.27 | 117.6 |

Thermogravimetric analysis (TGA) was used to determine the composition and the thermal stability of the composites prepared. The thermogravimetric analysis results show that the thermal stability of the composites was greatly changed due to the effect of metal oxides (please see Fig. S2). Fig. S2 indicates that in six samples, there was an obvious weight loss at the temperature around 100–150 °C, which is attributed to the loss of adsorbed water. It's followed by a second obvious weight loss at the temperature ranging from 200 to 600 °C, which is caused by thermal degradation of polypyrrole [20]. At last, the TGA curve reaches a steady state until the thermal degradation completed. Based on the TG analyses, the amount of PPy in PPy/$Fe_3O_4$, PPy/$Al_2O_3$, PPy/$Al_2O_{3(C)}$, PPy/$SiO_2$ and PPy/$SiO_{2(C)}$ were approximately calculated to be 14.3, 16.2, 45.1, 16.5 and 13.9 wt%, respectively, suggesting that the PPy/$Al_2O_{3(C)}$ composites contained more PPy than others, namely, PPy have better polymerization on the surface of $Al_2O_{3(C)}$. As a result, the metal oxides have extensive impact on the polymerization degree of PPy on their surface, further influence their loading of PPy on the metal oxides.

Fig. 2 presents SEM images of the composites prepared. All samples have granular structures and the pure PPy has the smallest particle sizes. Rougher surfaces are observed in the PPy/$SiO_{2(C)}$ and PPy/$Al_2O_{3(C)}$ composites than other composites, which were mainly affected by the metal oxides which with rough surface, and the ragged and rough morphology would be more favorable for the MB adsorption [33]. Therefore, the metal oxides also influence the morphology of their composites, further influencing their adsorption capacity to MB.

### 3.2. Adsorption characteristic investigation

#### 3.2.1. Effect of surface potential on the adsorption capacity

Fig. 3 shows Zeta potential values and the pH of zero point charge ($pH_{pzpc}$) of PPy, PPy/$Fe_3O_4$, PPy/$Al_2O_3$, PPy/$Al_2O_{3(C)}$, PPy/$SiO_2$ and PPy/$SiO_{2(C)}$. From the results, the $pH_{pzpc}$ of PPy, PPy/$Fe_3O_4$, PPy/$Al_2O_3$, PPy/$Al_2O_{3(C)}$, PPy/$SiO_2$ and PPy/$SiO_{2(C)}$ are about 10.46, 2.91, 10.10, 9.10, 10.11, 2.99, respectively, showing that different composites with different metal oxides have different potential values and $pH_{pzpc}$. Different metal oxides in different synthesis methods may have different surface feature as well as different type and number of functional groups on their surface, resulting in different $pH_{pzpc}$. The $pH_{pzpc}$ of their composites would be extensively influenced by their metal oxides, and revealed different $pH_{pzpc}$. PPy/$Fe_3O_4$ own lower $pH_{pzpc}$, and more negative charges would be carried on their surface in our experimental pH range, showing more potential to adsorb MB by electrostatic attraction than PPy. It is interesting that Zeta potential of PPy and five composites reached similar (around $-40 \sim -50$ mV) when

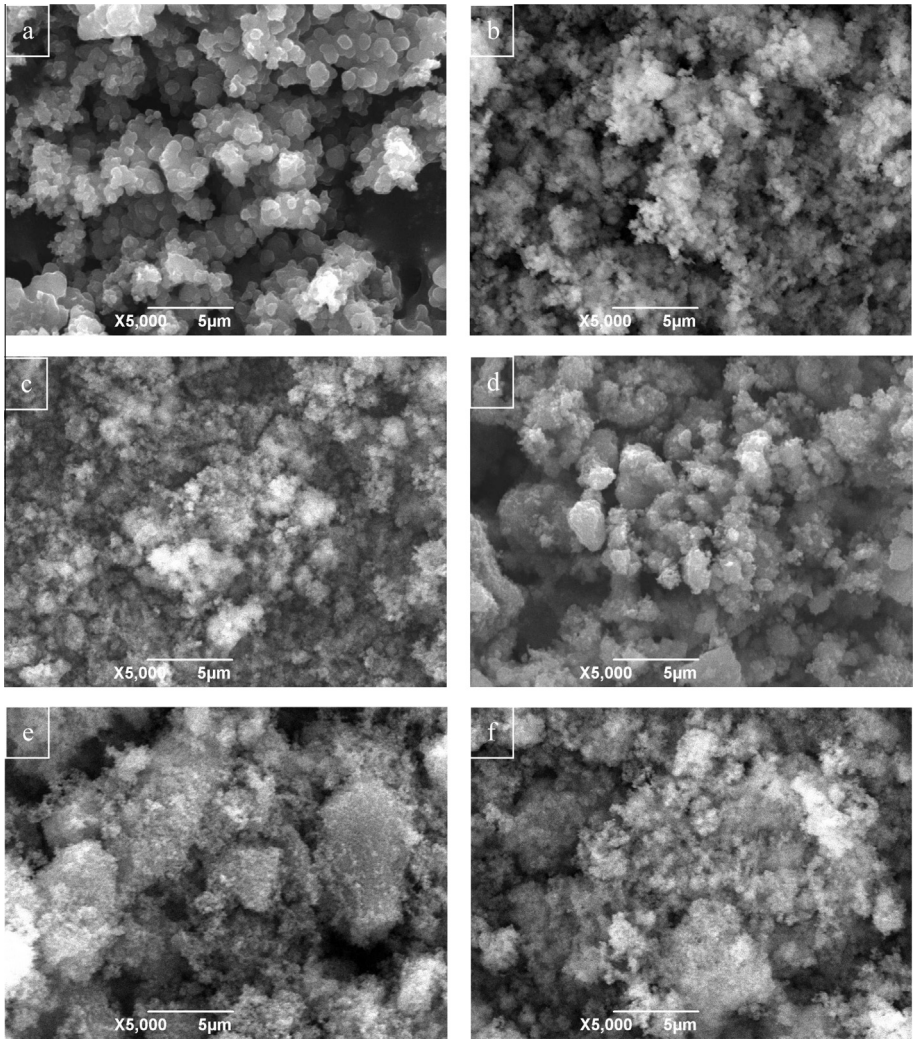


**Fig. 2.** SEM image of the (a) pure PPy, (b) PPy/$Fe_3O_4$, (c) PPy/$Al_2O_3$, (d) PPy/$Al_2O_{3(C)}$, (e) PPy/$SiO_2$, (f) PPy/$SiO_{2(C)}$ composites.

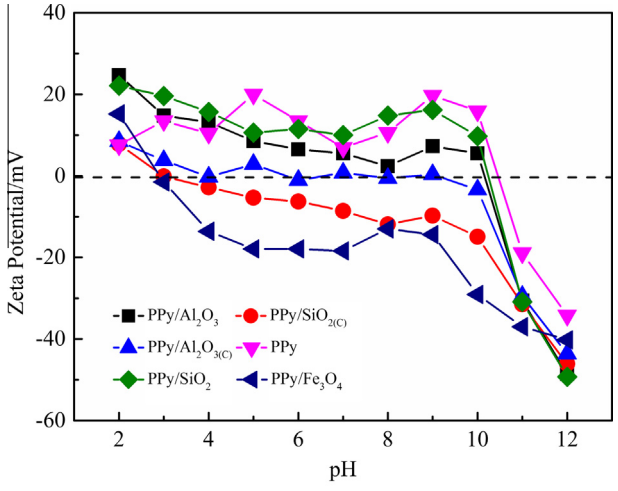


**Fig. 3.** Zeta potentials of the PPy/metal oxide composites (pH of pretreatment solution, 1, 2, 3, 4, 5, 6, 7, 8, 9, 10, 11, 12, 13; dosage, 5 mg; volume, 10 mL; ultrasonic vibrating, 30 min).

pH = 13, which was also found in literature [20]. And it may relate to properties of PPy. Ionic exchange may occur on the surface of PPy when composites were pretreated in a solution, and the composites may be positively or negatively charged according to the following equations,

$$PPyX + H^+ \leftrightarrow PPyXH^+$$

$$PPyX + OH^- \leftrightarrow PPyXOH^-$$

where X is the counter anions [34]. According to the Zeta potential results, these reaction may occur when the composites were pretreated in pH = 13 solution.

Effect of surface potential on the adsorption capacity is shown in Fig. 4. The adsorption capacity of all composites increased with the pH of the pre-preparation solution, and reached the largest at the pH of 13. This is because MB is a cationic dye, and it could be adsorbed easier or more difficult by the composites through electrostatic force when the composites were negatively or positively charged. As a result, the adsorption capacities of all composites increased with the pH. It can be noted that their adsorption capacity increased following a similar trend with pH even though they have completely different $pH_{pzpc}$, and their adsorption capacity boomed at pH = 13, meanwhile the composites still had adsorption capacity when the pH value of the pretreating solution was lower than the $pH_{pzpc}$. The similar results were also found in literatures [20,35]. It may be because that electrostatic attraction failed to be the first reason in adsorption when the pH of pretreatment solution was smaller than 13, and another adsorption mechanisms

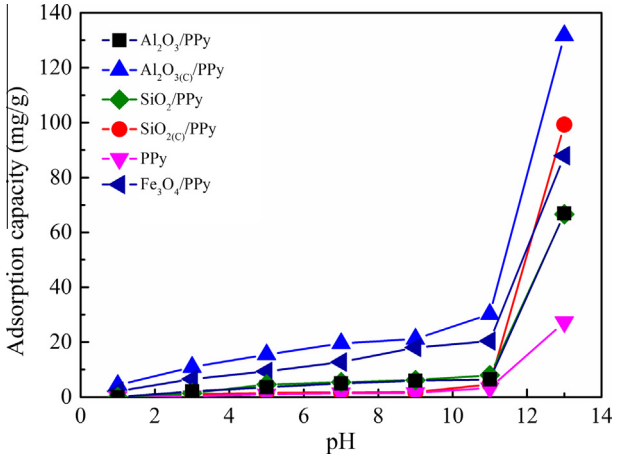


**Fig. 4.** Effect of surface potential on the adsorption capacity of MB onto the PPy/metal oxide composite (initial concentration, 300 mg/L; volume, 20 mL; contact time, 4 h; temperature, 25 °C; oscillator speed, 200 r/min; adsorbent dosage, 2.0 g/L; pH of pretreatment solution, 1, 3, 5, 7, 9, 11, 13).

such as hydrogen bonding, van der Waals interaction as well as physical sorption were coexisted, while the electrostatic attraction may play an important role in adsorption for MB when the pH of pretreatment solution was larger than 13 due to the negatively charged PPy. But it should be noted that the electrostatic attraction still existed if the pH of pretreatment solution lager than $pH_{pzpc}$ of composites. Thus, the adsorption capacity can be improved by treating samples with alkali solution (pH = 13).

### 3.2.2. Effect of ionic strength on the adsorption capacity

The salt in the dye solution has a great effect on the adsorption properties of adsorbents. Fig. 5 shows the results of effect of ionic strength on the adsorption capacity. According to the results, the adsorption capacity decreased with $Na_2SO_4$ concentration in the MB solution increased. These results are consistent with that reported before [20,34]. Zhang and Bai [34] and Lan et al. [36] indicated that the increase of ionic concentration would decrease the pore size of adsorbents and the amount of adsorption sites on the one hand, thus reducing the electrostatic interaction between the adsorbates and adsorbents and the adsorption capacity of adsorbents. However, the increase of ionic concentration would weaken the electrostatic repulsion between the adsorbates, and increase the adsorption capacity of adsorbents. The results show that these factors mention above eventually led to the decrease of adsorption capacity of the composites prepared, suggesting that the electrostatic repulsion as well as $Na^+$ competition between the adsorbates can be neglected in the adsorption process.

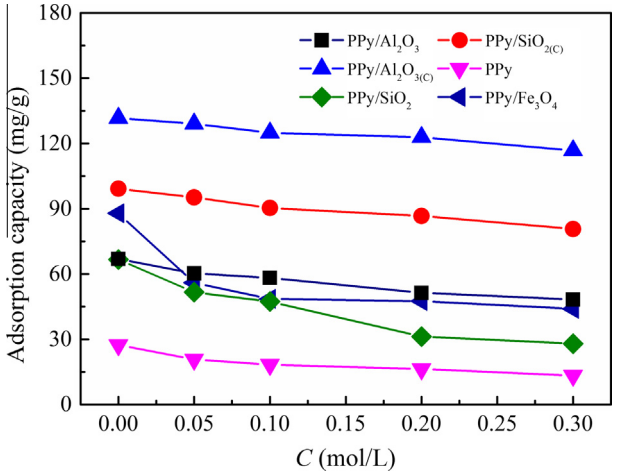


**Fig. 5.** Effect of ionic strength on the adsorption capacity of MB onto the PPy/metal oxide composite (initial concentration, 300 mg/L; volume, 20 mL; contact time, 4 h; temperature, 25 °C; oscillator speed, 200 r/min; adsorbent dosage, 2.0 g/L; concentration of $Na_2SO_4$, 0, 0.05, 0.1, 0.15, 0.2, 0.3 mol/L).

### 3.2.3. Adsorption isotherm

Adsorption isotherm was investigated to describe the balance and affinity between adsorbents and adsorbates as well as the adsorption ability of adsorbents. The linear forms of the Langmuir and Freundlich models listed above were used for modeling the adsorption isotherm data. The adsorption isotherm model fitting parameters are listed in Table 2. The results present that experimental results fit better to the Langmuir model ($R^2 > 0.99$), indicating that the adsorption of MB on the five PPy/metal oxide composites was monolayer. From the Langmuir fitting results, it's obvious that the addition of metal oxides greatly improved the adsorption capacity of PPy, and the $PPy/Al_2O_{3(C)}$ composite, whose adsorption capacity reaches 134.77 mg/g, has the best adsorption capacity, which is almost six time more than that of the pure PPy. The order of $q_m$ follows $PPy/Al_2O_{3(C)} > PPy/SiO_{2(C)} > PPy/Fe_3O_4 > PPy/SiO_2 > PPy/Al_2O_3 > PPy$, which was in accordance with the order of their $S_{BET}$. Higher $S_{BET}$ the composite was, more active adsorption sites the adsorbates available, resulting in higher adsorption capacity. Meanwhile, literature [33] pointed out that the ragged and rough morphology would be more favorable for the MB adsorption. Rougher surfaces are observed in the $PPy/SiO_{2(C)}$ and $PPy/Al_2O_{3(C)}$ composites than other composites, thus higher adsorption capacity were obtained. It is interesting that the order of $K_L$, which reveals the affinity between adsorbents and adsorbates [37], is $PPy/Al_2O_{3(C)} > PPy/Al_2O_3 > PPy/SiO_{2(C)} > PPy/SiO_2 > PPy/Fe_3O_4 > PPy$, showing an extensive benefit of metal oxides on MB affinity of PPy. Meanwhile, it can be deduced clearly that the affinity order of metal oxides for MB is $Al_2O_3 > SiO_2 > Fe_3O_4$, which haven't been investigated yet. It should be noted that $Al_2O_3$ may possess a plenty of surface hydroxyls, and the hydroxyls would have an important influence on the adsorption performance of its composite for MB, further influencing the adsorption capacity and affinity of its composite for MB. All in all, $PPy/Al_2O_{3(C)}$ composite has the most PPy, higher specific surface area, rougher surface, more adsorption sites available and high affinity with MB, stating as a promising adsorbent for MB.

According to literature [38], the slope (1/n) in the linear form of Freundlich isotherm reports the adsorption difficulty. If the slope (1/n) equals 0.1–0.5, it means the adsorption process is easy to achieve. If the slope (1/n) > 2, it means that the adsorbate is hard to be adsorbed. From the results of the linear form of Freundlich

**Table 2**
Adsorption equilibrium parameters acquired from the Langmuir, Freundlich models in the adsorption of MB onto PPy/metal oxide composites (initial concentration of MB, 50, 100, 150, 200, 250, 300, 350, 400 mg/L in PPy/metal oxides composites; initial concentration of MB, 10, 20, 30, 40, 50, 60, 70, 80 mg/L in PPy; volume, 20 mL; contact time, 3 h; temperature, 25, 35, 45 °C; oscillator speed, 200 r/min; adsorbent dose, 2.0 g/L; 1 mol/L NaOH pretreatment).

| Composites | Langmuir model | | | Freundlich model | | |
|---|---|---|---|---|---|---|
| | $q_m$ | $K_L$ | $R^2$ | 1/n | $K_F$ | $R^2$ |
| PPy | 27.82 | 0.06 | 0.996 | 0.23 | 34.4 | 0.868 |
| $PPy/Fe_3O_4$ | 92.08 | 0.15 | 0.996 | 0.13 | 41.9 | 0.957 |
| $PPy/Al_2O_3$ | 79.37 | 0.26 | 0.996 | 0.17 | 16.1 | 0.935 |
| $PPy/Al_2O_{3(C)}$ | 134.77 | 0.73 | 0.998 | 0.15 | 36.9 | 0.886 |
| $PPy/SiO_2$ | 91.83 | 0.20 | 0.997 | 0.17 | 69.8 | 0.959 |
| $PPy/SiO_{2(C)}$ | 104.71 | 0.23 | 0.997 | 0.22 | 18.7 | 0.950 |

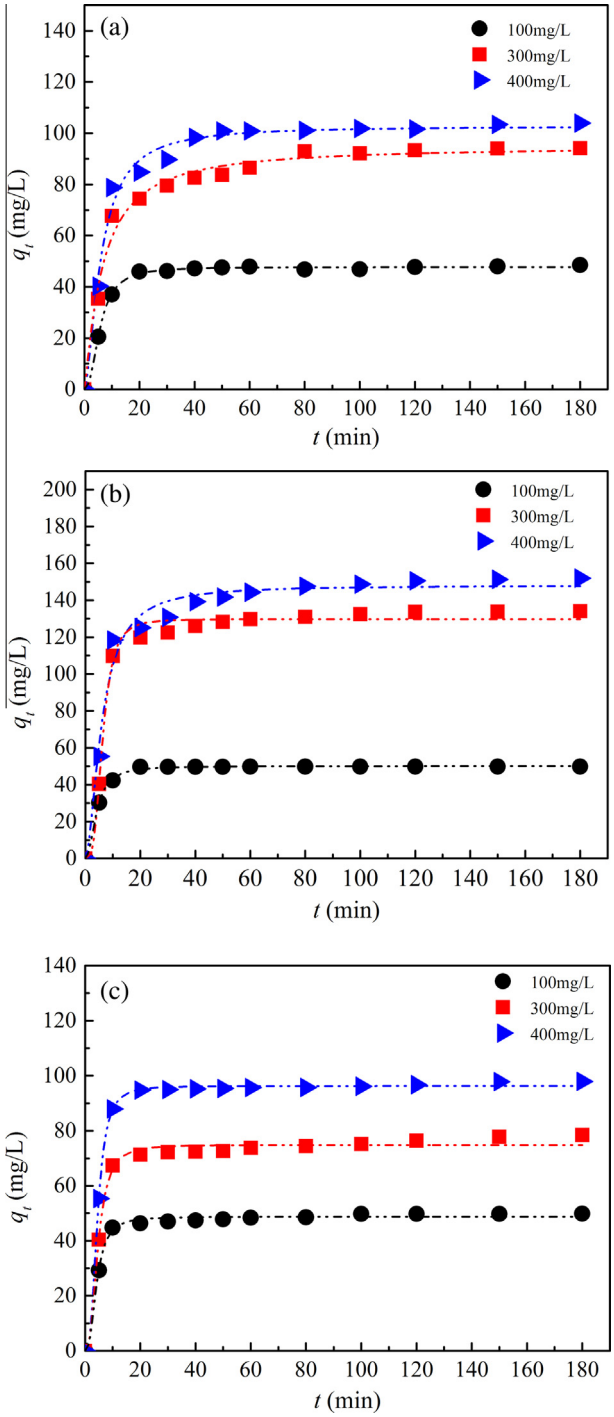


**Fig. 6.** Contact time versus the adsorption behavior for the adsorption of MB onto the (a) $PPy/SiO_{2(C)}$, (b) $PPy/Al_2O_{3(C)}$ and (c) $PPy/Fe_3O_4$ composites (initial concentration of MB, 100, 300, 400 mg/L; volume, 20 mL; contact time, 5, 10, 15, 20, 25, 30, 40, 50, 60, 80, 100, 120, 150, 180 min; temperature, 25 °C; oscillator speed, 200 r/min; temperature, 25 °C; adsorbent dosage, 2.0 g/L; 1 mol/L NaOH pretreatment).

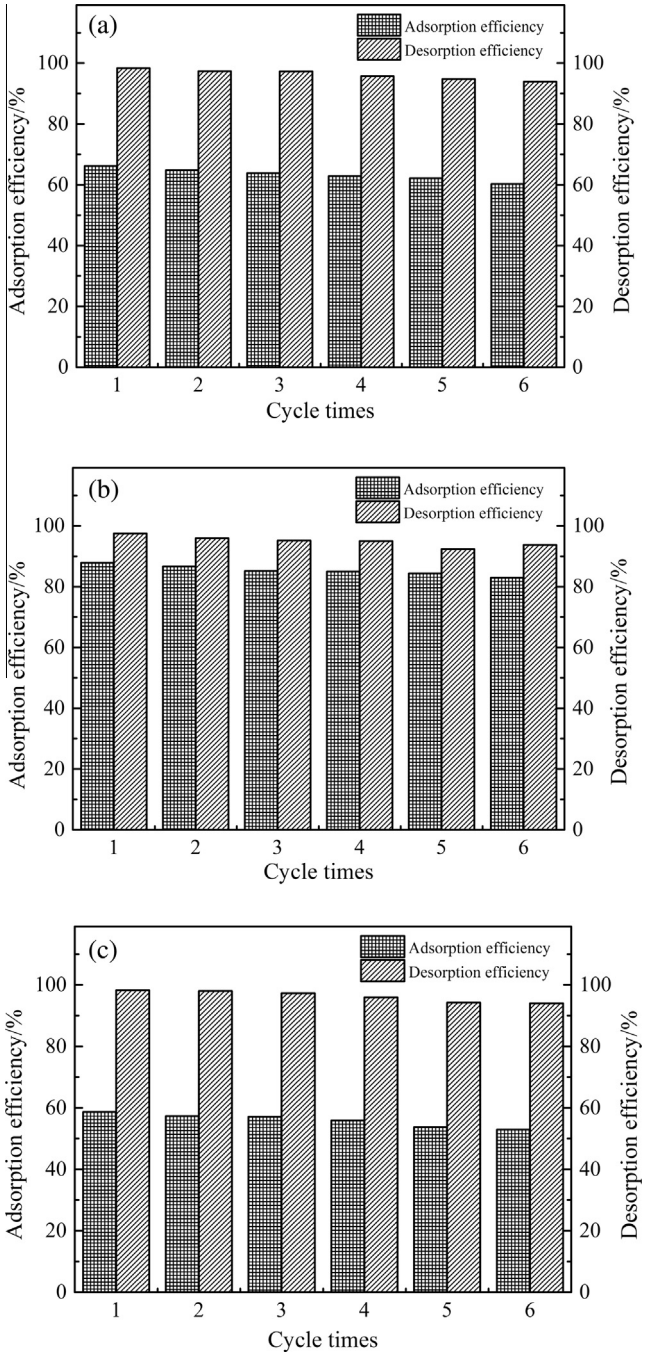


**Fig. 7.** Adsorption stabilities by HCl-elution and NaOH-activation method of the (a) $PPy/SiO_{2(C)}$, (b) $PPy/Al_2O_{3(C)}$ and (c) $PPy/Fe_3O_4$ composites (initial concentration, 300 mg/L; volume of MB solution, 20 mL; contact time, 3 h; temperature, 25 °C; oscillator speed, 200 r/min; adsorbent dosage, 2.0 g/L; recycle time, 6; c(HCl) = 1 mol/L; c(NaOH) = 1 mol/L; volume of HCl/NaOH solution, 20 mL).

isotherm, the slopes (1/n) are all less than 0.5, indicating that the adsorption for MB of the composites was favorable. The $K_F$, which relates to the adsorption capacity and adsorption affinity [39], further confirms that the affinity between PPy and MB were also greatly improved by composite with metal oxides. Three composites with higher adsorption capacity, namely $PPy/SiO_{2(C)}$, $PPy/Al_2O_{3(C)}$ and $PPy/Fe_3O_4$, were further applied for adsorption characteristic investigation.

### 3.2.4. Adsorption kinetic

The effect of contact time is shown in Fig. 6. In all samples, the adsorption capacity increases sharply in the first 10 min, and reaches the equilibrium after 60 min. The MB adsorption rate was fast in the first stage owning to the large number of adsorption sites and the high concentration gradient of MB. As the adsorption carried on, the adsorption sites and concentration gradient lost gradually, resulting to reduce of adsorption rate [25]. The kinetic data were fitted with the pseudo-first-order and pseudo-second-order model to describe the kinetic characteristic of the adsorption

**Table 3**
Kinetic parameters obtained from the pseudo-first-order and pseudo-second-order models of MB adsorption onto the (a) $PPy/SiO_{2(C)}$, (b) $PPy/Al_2O_{3(C)}$ and (c) $PPy/Fe_3O_4$ composites (initial concentration of MB, 100, 300, 400 mg/L; volume, 20 mL; contact time, 5, 10, 15, 20, 25, 30, 40, 50, 60, 80, 100, 120, 150, 180 min; temperature, 25 °C; oscillator speed, 200 r/min; temperature, 25 °C; oscillator speed, 200 r/min; adsorbent dose, 2.0 g/L; 1 mol/L NaOH pretreatment).

| $C_0$ ($mg\ L^{-1}$) | | $PPy/SiO_{2(C)}$ | | $PPy/Al_2O_{3(C)}$ | | $PPy/Fe_3O_4$ | |
|---|---|---|---|---|---|---|---|
| | | Pseudo-first-order sorption kinetics | Pseudo-second-order sorption kinetics | Pseudo-first-order sorption kinetics | Pseudo-second-order sorption kinetics | Pseudo-first-order sorption kinetics | Pseudo-second-order sorption kinetics |
| 100 | $R^2$ | 0.476 | 1.000 | 0.894 | 0.999 | 0.988 | 0.999 |
| | $K_i$ | 0.0047 | 0.031 | 0.010 | 0.04 | 0.017 | 0.024 |
| | $q_{e(L)}$ | 49.93 | 49.925 | 48.593 | 48.593 | 48.894 | 48.894 |
| | $q_{e(C)}$ | 2.87 | 49.850 | 0.29 | 48.473 | 3.23 | 49.020 |
| 300 | $R^2$ | 0.926 | 0.999 | 0.974 | 0.999 | 0.904 | 0.999 |
| | $K_i$ | 0.017 | 0.025 | 0.015 | 0.036 | 0.0072 | 0.016 |
| | $q_{e(L)}$ | 99.282 | 99.282 | 131.722 | 131.722 | 87.958 | 87.958 |
| | $q_{e(C)}$ | 52.34 | 97.943 | 33.55 | 136.426 | 12.28 | 79.177 |
| 400 | $R^2$ | 0.857 | 0.999 | 0.993 | 0.999 | 0.678 | 0.999 |
| | $K_i$ | 0.011 | $2.369 \times 10^{-3}$ | 0.012 | $2.010 \times 10^{-3}$ | 0.011 | $1.010 \times 10^{-3}$ |
| | $q_{e(L)}$ | 102.538 | 102.538 | 135.922 | 135.922 | 90.523 | 90.523 |
| | $q_{e(C)}$ | 25.38 | 106.496 | 44.76 | 156.006 | 9.59 | 98.328 |


**Fig. 8.** Photos of recyclability tested by a magnet: (a) before adsorption and (b) separation using a magnet after adsorption.

for MB of the composites. The kinetic model fitting parameters are listed in Table 3, and $R^2$ was used to describe the suitability of the model. The results suggested that the experimental results fitted well with the pseudo-second-order model. Additionally, $q_{e(C)}$, which were obtained in the pseudo-second-order model, were more close to the values obtained from experimentally or Langmuir fitting model ($q_{e(L)}$). As a result, it can be concluded that the adsorption rate for MB is controlled by the chemical sorption, which may involve electron sharing or electron transfer in the adsorption process between composites and adsorbates, rather than physical diffusion [40]. The order of $K_2$ is $PPy/Al_2O_{3(C)} > PPy/SiO_{2(C)} > PPy/Fe_3O_4$, further showing a fast adsorption and good affinity of $PPy/Al_2O_{3(C)}$ for MB.

### 3.2.5. Desorption and regeneration experiments

In a practical point, an excellent repeated availability of an adsorbent is crucial to its application. According to the results obtained from the study of effect of surface potential on the adsorption capacity, the composites are highly pH dependent. The adsorption capacity for MB of the composites are quite low, and the MB adsorbed could be released in low pH solution, while

**Table 4**
Adsorption capacity of various common adsorbents for MB.

| Adsorbents | Adsorption capacity for MB ($mg\ g^{-1}$) | Ref. |
|---|---|---|
| Melamine-g-$C_3N_4$ | 1.64 | [42] |
| Thiourea-g-$C_3N_4$ | 1.87 | [42] |
| Urea-g-$C_3N_4$ | 2.51 | [42] |
| Raw-chitin | 12.52 | [43] |
| Activated carbon | 15.59 | [44] |
| Seaweed-zinc oxide-PANi | 20.55 | [44] |
| Ultrasonic surface modified chitin | 26.69 | [43] |
| Carbon nanotube | 45.9 | [45] |
| Polyacrylic acid/$MnFe_2O_4$ | 53.3 | [45] |
| Activated montmorillonite | 64.43 | [46] |
| PANi hydrogel | 71.42 | [47] |
| $Fe_3O_4$/activated montmorillonite | 106.38 | [46] |
| $PPy/Al_2O_3$ | 79.37 | This study |
| $PPy/SiO_2$ | 91.86 | This study |
| $PPy/Fe_3O_4$ | 92.08 | This study |
| $PPy/SiO_{2(C)}$ | 104.71 | This study |
| $PPy/Al_2O_{3(C)}$ | 134.77 | This study |
| $Fe_3O_4$-xGO | 526.32 | [48] |
| Poly (AA co PVP)/PGS | 1775 | [49] |

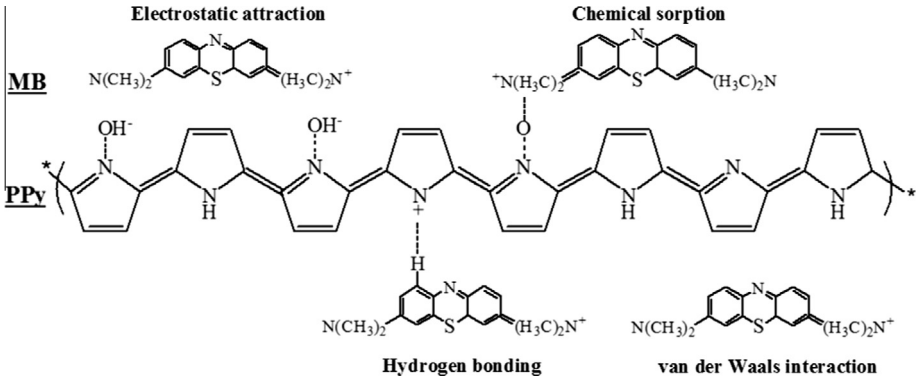


**Scheme 1.** The possible mechanism for the adsorption of MB from aqueous solution.

the good adsorption capacity of composites can be obtained in high pH solution, thus acquiring the possibility of regeneration of the composites. In this study, 1 mol/L HCl as the elution agent and 1 mol/L NaOH as the activator were applied to investigate the adsorption stabilities of the PPy/metal oxide composites. The results are depicted in Fig. 7. It showed that all the composites can be used for six cycles without significant adsorption capacity loss, concluding that the regeneration method by HCl-elution and NaOH-activation is available, and the three composites prepared own excellent stability and outstanding recycle possibility. Meanwhile, PPy/$Fe_3O_4$ can be collected using hand held magnet, showing a unique advance (Fig. 8).

*3.2.6. Comparison with other studied adsorbent*

The maximum adsorption capacity $q_m$ obtained from Langmuir model for MB of the composites prepared were compared with that of various common adsorbents reported as shown in Table 4. Even though the adsorption capacities of the as-prepared composites were lower than that of some material, the easier synthesis, faster adsorption, easier regeneration, higher adsorption capacity make the as-prepared composites more attractive to be an adsorbents for MB removal.

### 3.3. Adsorption mechanism discussion

It is well know that the cationic dye adsorption onto the adsorbents is mainly due to the electrostatic attraction [41]. In the study of effect of surface potential on the adsorption capacity, we found a property of the composites that some ion exchange occurred when the composites were pretreated in a solution with different pH, and the surface of PPy could be positively or negatively charged. Namely the surface of the adsorbent would carried positive charge when the Zeta potential below $pH_{pzpc}$, vice visa. This property lead to an electrostatic attraction between MB and the composites when the pH value of pretreating solution was higher than the $pH_{pzpc}$ and a decrease of the adsorption capacity of the composites for MB when the pH value of pretreating solution was lower than $pH_{pzpc}$ [20]. However, the composites still had adsorption capacity when the pH value of the pretreating solution was lower than the $pH_{pzpc}$, suggesting that another adsorption mechanism was coexisted. N atoms situating in the PPy matrix are highly electronegative, resulting that the composites could adsorb MB through hydrogen bonding [2,20]. Meanwhile, the experimental results fitted well with the pseudo-second-order model, hinting that the adsorption rate is controlled by the chemical sorption, which involves the electron sharing or electron transfer in the adsorption process between MB and the composites [40]. What's more, the van der Waals interaction can't be neglected as well [2]. The plausible adsorption mechanism of the composite for MB was proposed and shown in Scheme 1.

## 4. Conclusions

In short, pure polypyrrole and different metal oxides ($SiO_2$, $SiO_{2(C)}$, $Al_2O_3$, $Al_2O_{3(C)}$ and $Fe_3O_4$) coated with polypyrrole were successfully synthesized in this paper, and influence of metal oxides on various properties and the adsorption characteristic of their composites were investigated. The results indicated that the PPy content, textural properties, Zeta potential and morphology of composite, which have great impact on adsorption capacity for MB, were highly influenced by metal oxides. Meanwhile, the affinity of metal oxides with MB has great impact on that of their composites. The order of $K_L$ is PPy/$Al_2O_{3(C)}$ > PPy/$Al_2O_3$ > PPy/$SiO_{2(C)}$ > PPy/$SiO_2$ > PPy/$Fe_3O_4$ > PPy, confirming that $Al_2O_3$ owns outstanding affinity with MB than other two metal oxides. In the adsorption characteristic study, kinetic data of the composites selected (PPy/$SiO_{2(C)}$, PPy/$Al_2O_{3(C)}$ and PPy/$Fe_3O_4$) were described appropriately by the pseudo-second-order model, indicating that the chemisorption may be the rate limiting step. The order of $K_2$ is PPy/$Al_2O_3$ > PPy/$SiO_2$ > PPy/$Fe_3O_4$, further showing a fast adsorption and good affinity of PPy/$Al_2O_{3(C)}$ for MB. Results gained from the desorption and regeneration experiments suggested that the regeneration method by HCl-elution and NaOH-activation is available and the composites selected still owned dramatic adsorption and desorption efficiency after six adsorption-desorption cycles, making a promise that the composites especially PPy/$Al_2O_{3(C)}$ and PPy/$Fe_3O_4$ have a bright future in MB removal application. Furthermore, electrostatic attraction, hydrogen bonding, van der Waals interaction and chemical sorption involving the electron sharing or electron transfer may play important roles in the MB adsorption process of the PPy/metal oxide composites.

## Acknowledgements

The authors gratefully acknowledge the financial supports from the National Natural Science Foundation of China (Grant No. 21307098).

## Appendix A. Supplementary material

Supplementary data associated with this article can be found, in the online version, at http://dx.doi.org/10.1016/j.jcis.2016.04.017.

## References


[1] T. Wu, X. Cai, S. Tan, H. Li, J. Liu, W. Yang, Adsorption characteristics of acrylonitrile, p-toluenesulfonic acid, 1-naphthalenesulfonic acid and methyl blue on graphene in aqueous solutions, Chem. Eng. J. 173 (2011) 144–149.

[2] L. Yang, Y. Zhang, X. Liu, X. Jiang, Z. Zhang, T. Zhang, L. Zhang, The investigation of synergistic and competitive interaction between dye Congo red and methyl blue on magnetic $MnFe_2O_4$, Chem. Eng. J. 246 (2014) 88–96.

[3] W.H. Cheung, Y.S. Szeto, G. McKay, Enhancing the adsorption capacities of acid dyes by chitosan nano particles, Bioresour. Technol. 100 (2009) 1143–1148.

[4] K.G. Bhattacharyya, A. Sharma, Azadirachta indica leaf powder as an effective biosorbent for dyes: a case study with aqueous Congo Red solutions, J. Environ. Manage. 71 (2004) 217–229.

[5] S.M. Xu, J.L. Wang, R.L. Wu, J.D. Wang, H. Li, Adsorption behaviors of acid and basic dyes on crosslinked amphoteric starch, Chem. Eng. J. 117 (2006) 161–167.

[6] S. Duran, D. Solpan, O. Guven, Synthesis and characterization of acrylamide-acrylic add hydrogels and adsorption of some textile dyes, Nucl. Instr. Meth. Phys. Res. Sect. B – Beam Interact. Mater. Atoms 151 (1999) 196–199.

[7] M. Hongyang, C. Burger, B.S. Hsiao, B. Chu, Ultra-fine cellulose nanofibers: new nano-scale materials for water purification, J. Mater. Chem. 21 (2011) 7507–7510.

[8] G. Sen, S. Ghosh, U. Jha, S. Pal, Hydrolyzed polyacrylamide grafted carboxymethylstarch (Hyd. CMS-g-PAM): an efficient flocculant for the treatment of textile industry wastewater, Chem. Eng. J. 171 (2011) 495–501.

[9] A.R. Khataee, Photocatalytic removal of C.I. Basic Red 46 on immobilized $TiO_2$ nanoparticles: artificial neural network modelling, Environ. Technol. 30 (2009) 1155–1168.

[10] X.-C. Ruan, M.-Y. Liu, Q.-F. Zeng, Y.-H. Ding, Degradation and decolorization of reactive red X-3B aqueous solution by ozone integrated with internal micro-electrolysis, Sep. Purif. Technol. 74 (2010) 195–201.

[11] S.J. Allen, G. McKay, J.F. Porter, Adsorption isotherm models for basic dye adsorption by peat in single and binary component systems, J. Colloid Interf. Sci. 280 (2004) 322–333.

[12] D.H. Zhao, X.J. Liu, Z.X. Deng, M.L. Cao, X.L. Zhang, W. Yin, Y.H. Wu, Preparation of highly effective hybrid adsorbent by anionic dye wastewater and its use in cationic dye wastewater, J. Environ. Eng. – ASCE 140 (2014) 6.

[13] W. Tanthapanichakoon, P. Ariyadejwanich, P. Japthong, K. Nakagawa, S.R. Mukai, H. Tamon, Adsorption–desorption characteristics of phenol and reactive dyes from aqueous solution on mesoporous activated carbon prepared from waste tires, Water Res. 39 (2005) 1347–1353.

[14] P.C.C. Faria, J.J.M. Órfão, M.F.R. Pereira, Adsorption of anionic and cationic dyes on activated carbons with different surface chemistries, Water Res. 38 (2004) 2043–2052.

[15] X. Zhang, R.B. Bai, Adsorption behavior of humic acid onto polypyrrole-coated nylon 6,6 granules, J. Mater. Chem. 12 (2002) 2733–2739.

[16] S.K. Bajpai, V.K. Rohit, M. Namdeo, Removal of phosphate anions from aqueous solutions using polypyrrole-coated sawdust as a novel sorbent, J. Appl. Polym. Sci. 111 (2009) 3081–3088.

[17] M. Karthikeyan, K.K. Satheeshkumar, K.P. Elango, Removal of fluoride ions from aqueous solution by conducting polypyrrole, J. Hazard. Mater. 167 (2009) 300–305.

[18] P. Qibing, Q. Renyuan, Protonation and deprotonation of polypyrrole chain in aqueous solutions, Synth. Met. 45 (1991) 35–48.

[19] J. Chen, J. Feng, W. Yan, Facile synthesis of a polythiophene/$TiO_2$ particle composite in aqueous medium and its adsorption performance for Pb(ii), RSC Adv. 5 (2015) 86945–86953.

[20] J. Li, Q. Zhang, J. Feng, W. Yan, Synthesis of PPy-modified $TiO_2$ composite in $H_2SO_4$ solution and its novel adsorption characteristics for organic dyes, Chem. Eng. J. 225 (2013) 766–775.

[21] J. Li, J. Feng, W. Yan, Excellent adsorption and desorption characteristics of polypyrrole/$TiO_2$ composite for Methylene Blue, Appl. Surf. Sci. 279 (2013) 400–408.

[22] A.H. Chen, C.Y. Yang, C.Y. Chen, C.Y. Chen, C.W. Chen, The chemically crosslinked metal-complexed chitosans for comparative adsorptions of Cu (II), Zn(II), Ni(II) and Pb(II) ions in aqueous medium, J. Hazard. Mater. 163 (2009) 1068–1075.

[23] M. Xu, Y.S. Zhang, Z.M. Zhang, Y. Shen, M.J. Zhao, G.T. Pan, Study on the adsorption of $Ca^{2+}$, $Cd^{2+}$ and $Pb^{2+}$ by magnetic $Fe_3O_4$ yeast treated with EDTA dianhydride, Chem. Eng. J. 168 (2011) 737–745.

[24] T.-T. Li, Y.-G. Liu, Q.-Q. Peng, X.-J. Hu, T. Liao, H. Wang, M. Lu, Removal of lead (II) from aqueous solution with ethylenediamine-modified yeast biomass coated with magnetic chitosan microparticles: kinetic and equilibrium modeling, Chem. Eng. J. 214 (2013) 189–197.

[25] D.L. Zhao, G.D. Sheng, J. Hu, C.L. Chen, X.K. Wang, The adsorption of Pb(II) on $Mg_2Al$ layered double hydroxide, Chem. Eng. J. 171 (2011) 167–174.

[26] A.R. Kul, H. Koyuncu, Adsorption of Pb(II) ions from aqueous solution by native and activated bentonite: kinetic, equilibrium and thermodynamic study, J. Hazard. Mater. 179 (2010) 332–339.

[27] N.V. Blinova, J. Stejskal, M. Trchova, J. Prokes, M. Omastova, Polyaniline and polypyrrole: a comparative study of the preparation, Eur. Polym. J. 43 (2007) 2331–2341.

[28] X.M. Feng, Z.Z. Sun, W.H. Hou, J.J. Zhu, Synthesis of functional polypyrrole/prussian blue and polypyrrole/Ag composite microtubes by using a reactive template, Nanotechnology 18 (2007) 7.

[29] M. Bhaumik, T.Y. Leswifi, A. Maity, V.V. Srinivasu, M.S. Onyango, Removal of fluoride from aqueous solution by polypyrrole/$Fe_3O_4$ magnetic nanocomposite, J. Hazard. Mater. 186 (2011) 150–159.

[30] A. Gok, A.G. Yavuz, S. Sen, Preparation and characterization of poly(2-halogenaniline) composites with $Al_2O_3$, $SiO_2$, and red mud, Int. J. Polym. Anal. Charact. 12 (2007) 155–169.

[31] B. Tanhaei, A. Ayati, M. Lahtinen, M. Sillanpää, Preparation and characterization of a novel chitosan/$Al_2O_3$/magnetite nanoparticles composite adsorbent for kinetic, thermodynamic and isotherm studies of Methyl Orange adsorption, Chem. Eng. J. 259 (2015) 1–10.

[32] K. Cheah, M. Forsyth, V.T. Truong, Ordering and stability in conducting polypyrrole, Synth. Met. 94 (1998) 215–219.

[33] J.H. Du, G. Morris, R.A. Pushkarova, R.S. Smart, Effect of surface structure of kaolinite on aggregation, settling rate, and bed density, Langmuir: ACS J. Surf. Colloids 26 (2010) 13227–13235.

[34] X. Zhang, R.B. Bai, Surface electric properties of polypyrrole in aqueous solutions, Langmuir: ACS J. Surf. Colloids 19 (2003) 10703–10709.

[35] J. Li, J. Feng, W. Yan, Synthesis of polypyrrole-modified $TiO_2$ composite adsorbent and its adsorption performance on acid Red G, J. Appl. Polym. Sci. 128 (2013) 3231–3239.

[36] Q.D. Lan, A.S. Bassi, J.X. Zhu, A. Margaritis, A modified Langmuir model for the prediction of the effects of ionic strength on the equilibrium characteristics of protein adsorption onto ion exchange/affinity adsorbents, Chem. Eng. J. 81 (2001) 179–186.

[37] P.X. Sheng, Y.P. Ting, J.P. Chen, L. Hong, Sorption of lead, copper, cadmium, zinc, and nickel by marine algal biomass: characterization of biosorptive capacity and investigation of mechanisms, J. Colloid Interf. Sci. 275 (2004) 131–141.

[38] T.J.H. Vlugt, R. Krishna, B. Smit, Molecular simulations of adsorption isotherms for linear and branched alkanes and their mixtures in silicalite, J. Phys. Chem. B 103 (1999) 1102–1118.

[39] G. Bayramoğlu, M.Y. Arıca, Removal of heavy mercury(II), cadmium(II) and zinc(II) metal ions by live and heat inactivated *Lentinus edodes* pellets, Chem. Eng. J. 143 (2008) 133–140.

[40] Y.S. Ho, Second-order kinetic model for the sorption of cadmium onto tree fern: a comparison of linear and non-linear methods, Water Res. 40 (2006) 119–125.

[41] P. Sharma, N. Hussain, D.J. Borah, M.R. Das, Kinetics and adsorption behavior of the methyl blue at the graphene oxide/reduced graphene oxide nanosheet-water interface: a comparative study, J. Chem. Eng. Data 58 (2013) 3477–3488.

[42] B. Zhu, P. Xia, W. Ho, J. Yu, Isoelectric point and adsorption activity of porous g-$C_3N_4$, Appl. Surf. Sci. 344 (2015) 188–195.

[43] G.L. Dotto, J.M. Santos, I.L. Rodrigues, R. Rosa, F.A. Pavan, E.C. Lima, Adsorption of Methylene Blue by ultrasonic surface modified chitin, J. Colloid Interf. Sci. 446 (2015) 133–140.

[44] R. Pandimurugan, S. Thambidurai, Synthesis of seaweed-ZnO-PANI hybrid composite for adsorption of methylene blue dye, J. Environ. Chem. Eng. 4 (2016) 1332–1347.

[45] W. Wang, Z. Ding, M. Cai, H. Jian, Z. Zeng, F. Li, J.P. Liu, Synthesis and high-efficiency methylene blue adsorption of magnetic PAA/$MnFe_2O_4$ nanocomposites, Appl. Surf. Sci. 346 (2015) 348–353.

[46] J. Chang, J. Ma, Q. Ma, D. Zhang, N. Qiao, M. Hu, H. Ma, Adsorption of methylene blue onto $Fe_3O_4$/activated montmorillonite nanocomposite, Appl. Clay Sci. 119 (2016) 132–140.

[47] B. Yan, Z. Chen, L. Cai, Z. Chen, J. Fu, Q. Xu, Fabrication of polyaniline hydrogel: synthesis, characterization and adsorption of methylene blue, Appl. Surf. Sci. 356 (2015) 39–47.

[48] L. Cui, X. Guo, Q. Wei, Y. Wang, L. Gao, L. Yan, T. Yan, B. Du, Removal of mercury and methylene blue from aqueous solution by xanthate functionalized magnetic graphene oxide: sorption kinetic and uptake mechanism, J. Colloid Interf. Sci. 439 (2015) 112–120.

[49] C.X. Yang, L. Lei, P.X. Zhou, Z. Zhang, Z.Q. Lei, Preparation and characterization of poly(AA co PVP)/PGS composite and its application for methylene blue adsorption, J. Colloid Interf. Sci. 443 (2015) 97–104.